On the Mix-down Times of Dynamically Active Potential Vorticity Filaments

J. Gavin Esler [1]

Program in Atmospheres, Oceans and Climate, Massachusetts Institute of Technology

Lorenzo M. Polvani

Department of Applied Physics and Applied Mathematics, Columbia University

R. Alan Plumb

Program in Atmospheres, Oceans and Climate, Massachusetts Institute of Technology

Abstract.
A simple model is used to study the evolution of potential vorticity filaments, viewed in cross-section, subject to steady shear and deformation flows representative of the large-scale atmospheric circulation. It is found that the balanced, ageostrophic circulation induced by the anomalous potential vorticity can cause the evolution of a dynamically active filament to differ substantially from that of a dynamically passive filament in a similar background flow. It is suggested that estimates of the mix-down time of material contained in atmospheric filaments need to be corrected to allow for this effect.

Introduction

There is strong observational evidence for the transport of filaments of high potential vorticity (PV) air, both out of the polar vortex into midlatitudes in the winter stratosphere e.g. [*Waugh et al.*, 1994], and across the tropopause from the stratosphere into the troposphere e.g. [*Appenzeller et al.*, 1996]. Considerable attention has focussed on the impact of such transport on atmospheric chemistry [*Eduoard et al.*, 1996] and on the sensitivity of the chemistry to the 'mix-down' time of the filaments into the ambient air [*Tan et al.*, 1998]. (Here, 'mix-down' time will be defined as the mean time for the vertical scale of a tracer filament to be reduced to that scale at which molecular diffusion becomes important.) Estimates of mix-down time are vital to efforts to parameterise the effect on chemistry caused by the prolonged isolation of air parcels at scales below the grid-scales of chemical transport models [*Thuburn and Tan*, 1997].

Estimates of mix-down time in the stratosphere have recently been given by *Haynes and Anglade* [1997], and others [*Balluch and Haynes*, 1996; *Waugh et al.*, 1997].

However, the fact that the filaments may be dynamically active, because they have higher PV than the ambient flow, was not included in the models used to derive these estimates. In this paper we present numerical experiments showing the dynamical evolution of filaments of anomalous PV, viewed in cross-section, in simple vertical shear and horizontal deformation flows representative of large-scale atmospheric flows. A secondary, ageostrophic circulation (that scales with the filament width L) is found to alter the evolution compared with that of a passive filament. These experiments therefore give some insight into how estimates of mix-down time should be corrected. The effect of radiative damping on filaments is also discussed.

Model and Experiments

In the experiments presented here, we consider the effect of a large-scale background flow $\overline{\mathbf{v}} = (\overline{u}, \overline{v}, 0)$ with associated buoyancy $\overline{b}$, on the evolution of a two-dimensional PV filament which has a perturbation velocity field $\mathbf{v} = (u, v, w)$ and buoyancy field b. All time-dependent variables are independent of y (the along filament direction); hence $\mathbf{v}$ and b are functions of t, x and z only.

We solve the incompressible, Boussinesq, nonhydrostatic equations

$$\frac{d\mathbf{v}}{dt} + \mathbf{v}.\nabla\overline{\mathbf{v}} + f\mathbf{k} \times \mathbf{v} = -\nabla\phi + b\mathbf{k}, \qquad (1)$$

$$\frac{db}{dt} + \mathbf{v}.\nabla\overline{b} = 0, \qquad (2)$$

$$u_x + w_z = 0. \qquad (3)$$

The derivative $d/dt = \partial_t + (\overline{u}+u)\partial_x + w\partial_z$, (for remaining definitions see *Snyder et al.* [1993]). A streamfunction ψ is defined, so that $\psi_z = u$ and $-\psi_x = w$. The PV is given by

$$q = (\theta_0/g\rho_0)\left[f\mathbf{k} + \nabla \times (\overline{\mathbf{v}} + \mathbf{v})\right].\nabla\left(\overline{b} + b\right), \qquad (4)$$

where ρ_0 and θ_0 are the reference density and potential

[1]Now at DAMTP, University of Cambridge.

temperature. $N^2 = \bar{b}_z$ is the constant ambient static stability.

The numerical model used to integrate equations (1-3) is a pseudo-spectral model based on that of *Bartello* [1995]. The domain is periodic in the x-direction, with dimension $2\pi L$, and has rigid lids located at $z = 0, \pi H$. Two resolutions are used, the lower with 64×64 wavenumbers, (192×96 gridpoints), the higher with 128×128 wavenumbers (384×192). The boundary conditions used in the vertical direction are $b = u_z = v_z = w = 0$ on $z = 0, \pi H$.

In each experiment the initial conditions are derived by assuming the buoyancy and wind fields are in semi-geostrophic (SG) balance with the filament PV, given by δq. Following *Snyder et al.* [1993], and taking suitably small aspect and Prandtl ratio ($H/L = f/N = 1/150$), $b = \phi_z^{SG}$ and $v = \phi_x^{SG}$ are obtained from δq through the equation

$$f^2 \phi_{zz}^{SG} + N^2 \phi_{xx}^{SG} + \phi_{xx}^{SG} \phi_{zz}^{SG} - (\phi_{xz}^{SG})^2 = \delta q \, \rho_0 f g / \theta_0, \quad (5)$$

subject to $\phi_z^{SG} = 0$ on the boundaries. The ageostrophic streamfunction ψ is then obtained from the Sawyer-Eliassen equation

$$(N^2 + \phi_{zz}^{SG})\psi_{xx} - 2\phi_{xz}^{SG}\psi_{xz} + (f^2 + \phi_{xx}^{SG})\psi_{zz} =$$

$$\begin{cases} -2\Lambda \phi_{xx}^{SG} & \text{for the shear flow} \\ -2\Gamma \phi_{xz}^{SG} & \text{for the deformation flow.} \end{cases} \quad (6)$$

As ψ is linear in either the shear Λ or the deformation rate Γ, filaments in an SG balanced flow with the same initial geometry will evolve in a self-similar fashion, on a time-scale $Nf^{-1}\Lambda^{-1}$ (shear case) or Γ^{-1} (deformation case), for any value of Λ or Γ. By nondimensionalising (5) it can be seen that the filament evolution is also independent of its absolute scale L.

The initial fields, for filaments with $\delta q = 2$ background PV units (or BPVU, where 1 BPVU $\equiv 1 \times \theta_0 g^{-1}\rho_0^{-1} f N^2$), are shown in Figure 1. In the case of deformation flow or weak shear, the background PV is given by 1BPVU, so $\delta q=2$BPVU corresponds to a filament with PV 3× the background value. This filament therefore has a higher relative PV compared to most of those observed in the winter stratosphere (0.5-1.5BPVU) [*Waugh et al.*, 1994], but lower than some of the stratospheric PV streamers observed in the upper troposphere (2-4BPVU) [*Appenzeller et al.*, 1996].

The Shear Flow Problem

In a simple balanced shear flow the background state is given by $\bar{u} = \Lambda z$, $\bar{v} = 0$ and $\bar{b} = -f\Lambda y + N^2 z$. For the adiabatic, inviscid experiment to be described we take $\Lambda = 0.1N$. This corresponds to a moderate shear in either the stratosphere or troposphere, but provided SG balance is valid the filament will evolve in a self-similar fashion at any Λ (see above).

Equations (1-3) are numerically integrated using this background state at high resolution. In order to suppress advection of the background temperature gradient
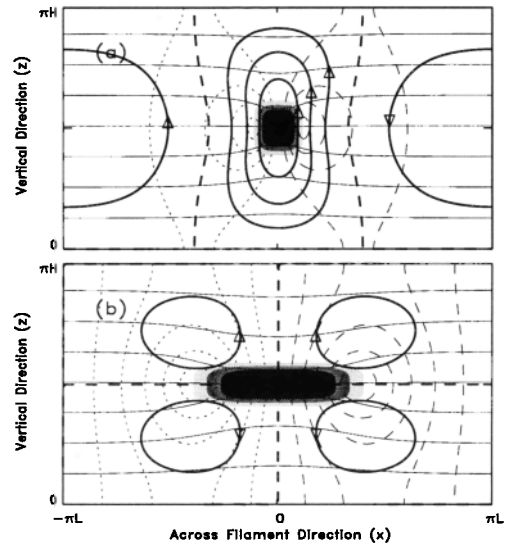

Figure 1. Initial conditions for (a) The shear flow case. (b) The deformation flow case. ($\delta q = 2$ BPVU.) Filled contours show filament PV, c.i. 0.5BPVU. Thin solid contours show total buoyancy $b + \bar{b}$, c.i. $0.4N^2H$. Thin dashed contours show positive v, dotted-negative v, c.i. $0.05fL$. Thick solid contours show ψ, c.i. $0.004\ fHL$. Thick dashed curve is $\psi = 0$.

on the boundaries (and therefore prevent the growth of Eady-type waves), a boundary heating term is added to the right hand side of (2). This has the form $Q^b = -H^b(z)\Lambda v$, where $H^b(z) = (1 - z/z_b)^2$ for $z < z_b = 0.1\pi H$, in the lower boundary region, and has similar structure on the upper boundary. A y-momentum forcing term F^b is also included, to minimise spurious PV generation. This satisfies $F_x^b = -(Q_z^b - \overline{Q^b}_z)$, where the overbar denotes a zonal mean ($\overline{F^b} = 0$).

Figure 2a and 2b show snapshots from the experiment at $t = 2Nf^{-1}\Lambda^{-1}, 4Nf^{-1}\Lambda^{-1}$. The ageostrophic circulation increases the rate of stretching of the filament (shaded region), relative to the evolution of a passive filament in the same background shear flow (thick solid contour). In particular, it is notable that the vertical velocity w (thin contours) maximises at the edges of the filament, advecting them into stronger horizontal winds. The limiting factor in the stretching process appears to be the geometry of the filament itself: the ageostrophic circulation weakens considerably as the filament is stretched out, so that it eventually behaves like a passive filament. Similar experiments with $\delta q = 1$BPVU and 4BPVU resulted in 55% and 170% increased stretching relative to the passive tracer by $t = 4Nf^{-1}\Lambda^{-1}$ respectively, compared to 115% in this case ($\delta q = 2$BPVU).

The integration was validated with the following tests. (1) Conservation of total PV: The final filament PV (at $t = 4Nf^{-1}\Lambda^{-1}$) was found to be 99.63% of the original. (2) Independence of numerical resolution: A low resolution experiment was carried out, and the filament was found to evolve in identical fashion, although PV conservation was poor near the end of the calculation.
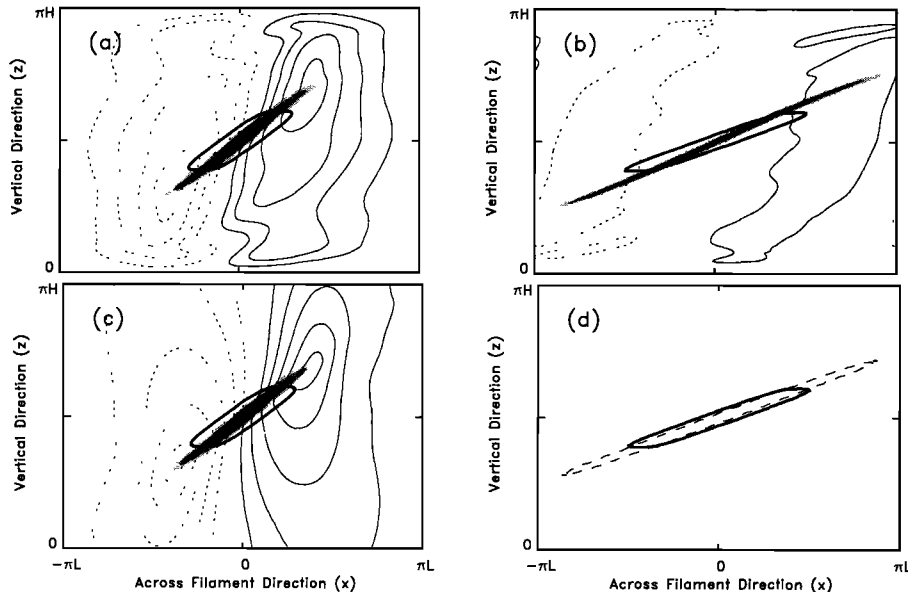
Figure 2. Snapshots for shear flow experiments (a) $t = 2N\Lambda^{-1}f^{-1}$. (b) $t = 4N\Lambda^{-1}f^{-1}$. (c) Double domain experiment $t=2N\Lambda^{-1}f^{-1}$. (d) Radiation experiment $t = 4N\Lambda^{-1}f^{-1}$. Filled contours show filament PV, c.i. 0.5BPVU. Thin contours show vertical velocity w (solid-positive, dotted-negative values), c.i. $0.0025fH$. Thick solid contour shows position of passive filament advected by basic flow (compare with 0.5BPVU contour). Dashed contour in (d) shows position of tracer advected by full flow.

(3) Independence of domain size: In order to ensure that the size of the domain, and in particular the boundary forcing, did not influence the outcome of the experiment, an low resolution experiment with double the domain size is presented. A snapshot from this experiment is shown in Figure 2c. Compared to Figure 2a, it is notable that the ageostrophic circulation penetrates into the extended domain, and the magnitude of the vertical velocity in the region of the filament is stronger by around 10%. The final shape of the filament is only slightly affected by this difference.

(4) Validation of SG balance: SG balance is formally valid only in the limit $\Lambda \rightarrow 0$. The model PV was inverted at intervals to compare the model fields to the SG balanced fields [*Snyder et al.*, 1993]. Good agreement was found in this experiment, and for experiments with Λ up to $\approx 0.5N$.

The Effect of Radiation

Haynes and Ward [1993] suggest a simple parameterisation of the effect of radiation on temperature anomalies in the stratosphere. At around 30mb, the scale-dependent thermal damping rate is approximately given (in days^{-1}) by $\alpha(m) = 0.05 + 0.125m^{1/2}$, where m is the vertical wavenumber in km^{-1}. This scheme is easily added to our model. If the vertical scale of the filament is such that the radiative timescale $\alpha^{-1}(2\pi/H)$ is very much shorter than the dynamical timescale, then the PV in the filament will be quickly dissipated by thermal damping, and the material within it will be advected by the large-scale flow as a passive tracer. Here we consider a shear flow case where $\alpha^{-1}(2\pi/H)$ is comparable to $N/f\Lambda$, by setting $\Lambda = 0.1N$, $H = 0.02$km and

$f = 10$days^{-1}. The final snapshot ($t = 4Nf^{-1}\Lambda^{-1}$) from this (low resolution) experiment is shown in Figure 2d. At this time the PV has been almost entirely dissipated, and as a result there is no longer a significant ageostrophic circulation. The dashed line shows the final boundary of the fluid originally contained within the PV filament. The presence of the ageostrophic circulation in the early stages of the experiment has still resulted in 95% greater elongation relative to a passive filament (solid curve).

The Deformation Flow Problem

In the deformation flow problem the background state is given by $\bar{u} = -\Gamma x$, $\bar{v} = \Gamma y$ and $\bar{b} = N^2z$. As in the shear flow problem, the initial state is determined by SG balance, see Figure 1b. (A broader initial filament is used to emphasise the effect of the ageostrophic flow.) A deformation rate of $\Gamma = 0.1f$ is taken as representative of the lower stratosphere. In the numerical model, the basic flow is reduced to zero in a thin boundary (10 grid points) on each side of $x = \pm\pi L$. Low resolution is used. Figure 3 shows a close-up snapshot of the filament ($t= 2\Gamma^{-1}$). The filament has been elongated in the y-direction by the basic flow, and the ageostrophic circulation has had the effect of further compressing the filament in the x-direction and increasing its vertical scale relative to that of a passive filament.

Conclusions

The ageostrophic circulation associated with a PV filament is found to accelerate the reduction in its vertical scale in a steady shear flow, and to accelerate the reduc-
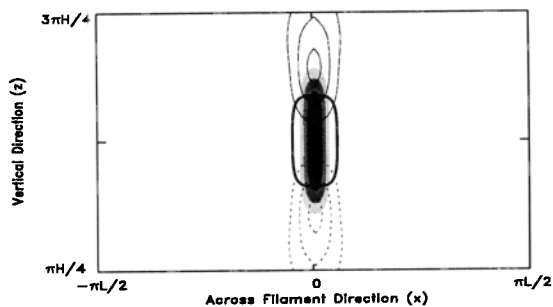
Figure 3. As Fig. 2 but close-up snapshot of deformation flow experiment ($t = 2\Gamma^{-1}$, δq=2BPVU.)

tion in its horizontal scale in a steady deformation flow. Some account of the ageostrophic circulation therefore needs to be taken if one is calculating the mix-down time of the material originally contained within an atmospheric PV filament. Table 1 shows the additional time taken for the passive filament to reach the relevant scale of the active filament (with $\delta q = $ 2BPVU) at the end of each experiment. A range of different initial geometries is shown. The additional time may be interpreted as the correction to mix-down time, and typical values for stratospheric parameters are also given. Filaments that are 'flat' (relative to the Prandtl ratio f/N) feel the effect of the ageostrophic circulation much more than those that are tall or tilted. This is an important point as numerical experiments [*Polvani and Saravanan*, 1999] often show tall sheets of PV stripped from vortices, although direct LIDAR measurements [*Plumb et al.*, 1994] have shown stratospheric filaments with vertical to horizontal scale ratios closer to f/N. In the case of filaments with small vertical scales, or those in weak background flows, radiative damping may also remove PV too quickly for the ageostrophic circulation to act. It is also far from clear how these results translate to the case when the background flow is unsteady, as in the atmosphere. Finally, it will be necessary to extend these experiments to three-dimensions, and determine how the roll-up of the PV filaments [*Waugh and Dritschel* 1999; *Polvani and Saravanan*, 1999] alters the results presented here.

Table 1. The extra time necessary for a passive filament to reach the same scale as an active filament (δq=2BPVU) in the experiments with different filament geometry. Ratios are filament scales relative to f/N. The tilted filament is the tall one rotated 45° in the direction of the shear. We take f^{-1}=0.1days.

Filament Geometry	Times for Shear Flow $(N\Lambda^{-1}f^{-1})$	Example Times $\Lambda = 0.05N$	Times for Deformation Flow (Γ^{-1})	Example Times $\Gamma = 0.03f$
Tall 4:1	1.3	2.6 days	0.25	0.8 days
Square 1·1	4.5	9 days	0.4	1.3 days
Flat 1:4	11.5	23 days	0.7	2.3 days
Tilted	1.8	3.6 days	0.2	0.7 days

References

Appenzeller C., H. C. Davies and W. A. Norton, Fragmentation of stratospheric intrusions, J. Geophys. Res., *101(D1)*, 1435-1456, 1996.

Balluch M. G. and P. H. Haynes, Quantification of lower stratospheric mixing processes using aircraft data, J. Geophys. Res., *102(D19)*, 23,487-23,504, 1997.

Bartello, P., Geostrophic adjustment and inverse cascades in rotating stratified turbulence, J. Atmos. Sci., *52*, 4410-4428, 1995.

Eduoard S., B. Legras, and V. Zeitlin, The effect of dynamical mixing in a simple model of the ozone hole, J. Geophys. Res., *101(D11)*, 16711-16788, 1996.

Haynes, P. H. and J. Anglade, The vertical-scale cascade in atmospheric tracers due to large-scale differential advection, J. Atmos. Sci., *54*, 1121-1136, 1997.

Haynes, P. H. and W. E. Ward, The effect of realistic radiative transfer on potential vorticity structures, including the influence of background shear and strain, J. Atmos. Sci., *50*, 3431-3453, 1993.

Plumb, R. A. and Coauthors, Intrusions into the lower stratospheric Arctic vortex during the winter of 1991-1992, J. Geophys. Res., *99(D1)*, 1089-1105, 1994..

Polvani, L.M. and R. Saravanan, The three-dimensional structure of breaking Rossby waves in the polar wintertime stratosphere, J. Atmos. Sci., submitted, 1999.

Snyder C., W. C. Skamarock and R. Rotunno, Frontal Dynamics near and following frontal collapse, J. Atmos. Sci., *50*, 3194-3211, 1993.

Tan D. H. G., P. H. Haynes, A. R. Mackenzie and J. A. Pyle, Effects of fluid-dynamical stirring and mixing on the deactivation of stratospheric chlorine, J. Geophys. Res., *103(D1)*, 1586-1605, 1998.

Thuburn J. and D. G. H. Tan, A parameterization of mix-down time for atmospheric chemicals, J. Geophys. Res., *102(D11)*, 13037-13049, 1997.

Waugh D. W. and Coauthors, Transport out of the lower stratospheric Arctic vortex by Rossby wave breaking, J. Geophys. Res., *99(D1)*, 1071-1088, 1994.

Waugh D. W. and Coauthors, Mixing of polar vortex air into middle latitudes as revealed by tracer-tracer scatterplots, J. Geophys. Res., *102(D11)*, 13119-13134, 1997.

Waugh D. W. and D. G. Dritschel, Vertical Structure of Rossby wave breaking: dependence on polar vortex vertical structure, J. Atmos. Sci., to appear, 1999.

J. G. Esler, Centre for Atmospheric Sciences, DAMTP, University of Cambridge, Silver St, Cambridge, CB3 9EW. United Kingdom. (e-mail: J.G.Esler@damtp.cam.ac.uk)

L. M. Polvani, Department of Applied Physics and Applied Mathematics, Columbia University, New York, NY 10027.

R. A. Plumb, Program in Atmospheres, Oceans and Climate, Massachusetts Institute of Technology, Cambridge, MA 02139.